

On friction and surface cracking during sliding of ice on ice

MAURINE MONTAGNAT, ERLAND M. SCHULSON

Thayer School of Engineering, Dartmouth College, Hanover, New Hampshire 03755-8000, U.S.A.

E-mail: erland.schulson@dartmouth.edu

ABSTRACT. As a complement to earlier measurements on the friction of both granular fresh-water ice and S2 columnar salt-water ice, new experiments were performed on the friction of S2 columnar fresh-water ice sliding against itself at low velocities (5×10^{-7} to $5 \times 10^{-1} \text{ m s}^{-1}$) and at -10°C , using the same double-shear device as was used earlier. The results showed that under a given set of experimental conditions the kinetic coefficient of friction of S2 fresh-water ice compares favorably with that of the other two variants. The experiments also revealed friction-induced surface cracks and recrystallized grains. These deformation features are explained, respectively, in terms of fracture mechanics and an earlier model of dynamic recrystallization in ice.

1. INTRODUCTION

Friction of ice against ice at low sliding velocities plays an important role in the brittle compressive failure of ice (Schulson, 2001) on scales small (laboratory) and large (Arctic Ocean). It is also important in the development of rafts and pressure ridges within the pack ice of the Arctic Ocean (Hopkins and others 1991, 1999). In an attempt to add to the existing body of knowledge of this phenomenon (Bowden and Hughes 1939; Barnes and others 1971; Evans and others 1976; Tusima 1977) Kennedy and others (2000) measured the kinetic coefficient of friction, μ , for fresh-water granular ice and for S2 columnar saline ice with a salinity of $4.3 \pm 0.2\text{‰}$, sliding against themselves at low speeds (5×10^{-7} to $5 \times 10^{-1} \text{ m s}^{-1}$) and elevated temperature (-40 to -3°C). They found that μ generally decreases with increasing sliding velocity and with increasing ambient temperature, but that μ is relatively insensitive to both pressure and grain-size over the ranges investigated (normal contact pressures $0.007\text{--}1\text{ MPa}$; grain-size $2\text{--}6 \text{ mm}$). The friction coefficients for the fresh-water and the saline ice were almost indistinguishable at high temperatures (-3° and -10°C), while at -40°C the friction of saline ice was about 15% lower than that of fresh-water ice. Kennedy and others (2000) interpreted their results in terms of creep, fracture and frictional melting, and on this basis were able to account reasonably well for the general behavior and for the small difference between the two kinds of ice at the lowest temperature.

In performing this work, Kennedy and others (2000) did not measure the friction of S2 columnar fresh-water ice against itself, leaving open the question as to whether this variant (from which river ice is made) would lead to a significant difference in results. In the interests of completion, this case is addressed in the present paper. We show that the friction coefficient of S2 fresh-water ice is essentially the same as that of the other two variants, at least at -10°C and at low velocities. Also, we present some new observations of cracks and recrystallized grains that were created during sliding.

2. EXPERIMENTAL PROCEDURE

To perform the experiments, we used the double-shear device that Kennedy and others (2000) developed (Fig. 1). Here we give only a summary of its main characteristics.

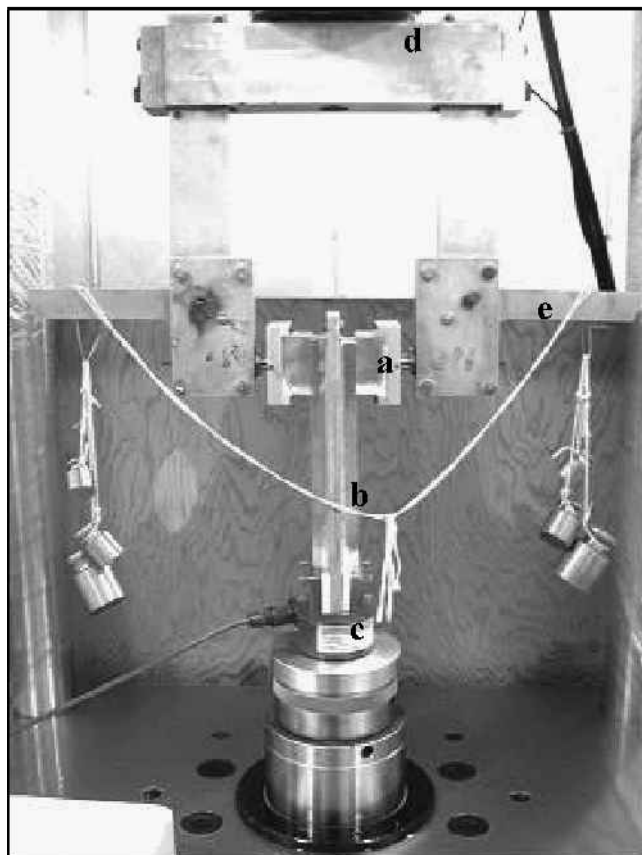


Fig. 1. Friction-testing apparatus: (a) stationary ice block; (b) mobile ice plates; (c) load transducer mounted on hydraulic actuator; (d) framework of testing apparatus; and (e) lever arms for normal loading of blocks. From Kennedy and others (2000).

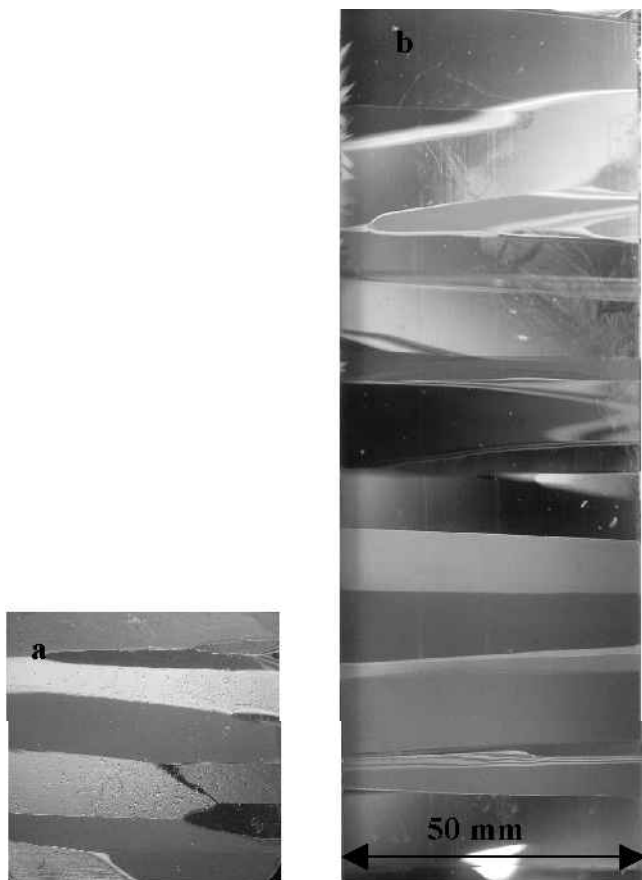


Fig. 2. Thin sections of S2 fresh-water ice showing (a) a stationary slab fixed on the apparatus on which the normal load is applied, and (b) a moving slab attached to the actuator (in vertical movement), on the load cell measuring the friction force.

An attachment was adapted to a servohydraulic, uniaxial material testing system (MTS). Constant normal force was applied to opposing faces of blocks of ice. Larger slabs ($220 \times 70 \text{ mm}^2$ in surface area; thickness $\leq 20 \text{ mm}$) were bonded to aluminum plates that were attached to the MTS actuator. A load cell (sensitivity 0.5 kg m s^{-2}) was mounted to the actuator which provided the desired velocity. Two laterally loaded and smaller slabs of ice ($50 \times 50 \text{ mm}^2$ in surface area; thickness $\leq 20 \text{ mm}$) were placed in contact with the larger slabs, but remained stationary during sliding. To provide good contact between the stationary and moving plates, the smaller stationary slabs were free to rotate around a horizontal axis, which was perpendicular to the sliding direction. Experiments were also done using non-rotating slabs, and the results were essentially the same.

To compare with the results of Kennedy and others (2000), samples were made from fresh-water S2 ice which was grown by unidirectionally freezing filtered and deionized Hanover tap water. S2 ice, as defined by Michel and Ramseier (1971), is characterized by columnar-shaped grains whose crystallographic c axes are more or less perpendicular to the long axes of the grains and randomly oriented within the plane normal to these long axes. Samples were positioned such that the long axes of the columnar grains of the larger (moving) and the smaller (stationary) slabs were parallel to the rubbing surface and perpendicular to the sliding direction (Fig. 2). Unless otherwise noted, the grain-size (taken as the average column diameter) was 6–8 mm. Following Kennedy and others (2000), the surfaces of the samples were prepared using a Leitz 1400 sledge-based microtome.

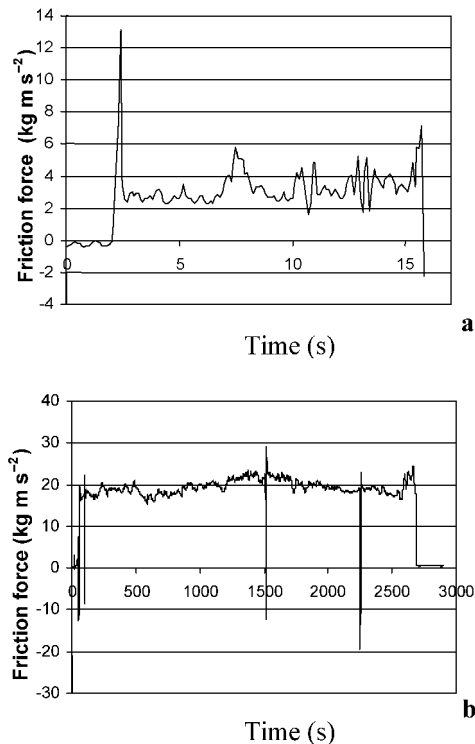


Fig. 3. Friction force vs time. The normal load is 25 kg m s^{-2} . (a) Sliding velocity of 10^{-2} m s^{-1} ; (b) sliding velocity of $5 \times 10^{-5} \text{ m s}^{-1}$.

A test consisted of a single pass of the opposing slabs in the direction of microtoming. The data collected included displacement and friction load as a function of time. Eight different sliding velocities were used, between $5 \times 10^{-6} \text{ m s}^{-1}$ and 10^{-2} m s^{-1} . Unless otherwise noted, the normal force applied on each stationary slab was kept at 25 kg m s^{-2} . This corresponded to an average stress of 0.01 MPa normal to the sliding surface, which is comparable to the lowest values used by Kennedy and others (2000). The experiments were run at a temperature of -10°C ($\pm 2^\circ\text{C}$).

3. RESULTS AND OBSERVATIONS

Figure 3 shows representative plots of friction force vs time for the sliding velocities of 10^{-2} m s^{-1} and $5 \times 10^{-5} \text{ m s}^{-1}$. The curves were generally characterized by an initial peak of varying amplitude, corresponding to static friction behavior, and by drops and rises in load which are indicative of stick-slip behavior. Large drops at 100, 1500 and 2200 s in Figure 2b were caused by localized uneven movements of the actuator.

At least four tests were performed for each condition. Exceptions are for the two lowest velocities, where three tests were performed at $v = 10^{-5} \text{ m s}^{-1}$ and only one at $v = 5 \times 10^{-6} \text{ m s}^{-1}$. Following Kennedy and others (2000), the kinetic friction coefficient was calculated using the relationship $\mu = F/2P$, where F is the measured friction force and P is the normal force applied on each stationary slab; the factor of two arises because two stationary slabs are pushed against the two faces of the moving slab. For each test, an average value F_t was obtained over the part of the load-time curve corresponding to a “kinematical” friction behavior. The average friction coefficient for each velocity was calculated over the F_t values ($\mu = \langle \mu_t \rangle$, where $\mu_t = F_t/2P$). The standard

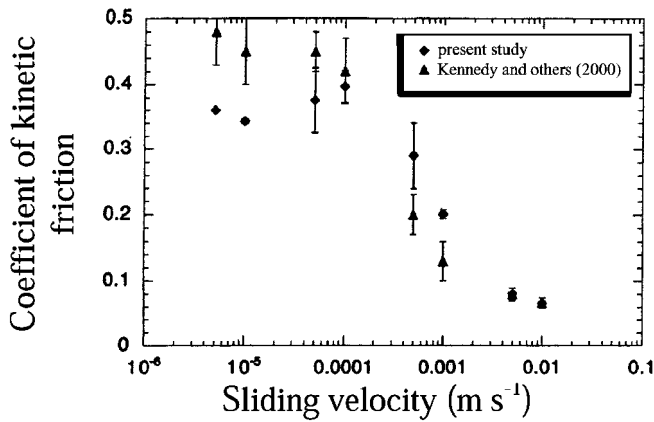


Fig. 4. Comparison of results by Kennedy and others (2000) for granular fresh-water ice (grain-size 4 mm) at a normal stress of 0.02 MPa, with the results obtained here for columnar S2 fresh-water ice (grain-size 6–8 mm) for a normal stress of 0.01 MPa at $T = -10^{\circ}\text{C}$.

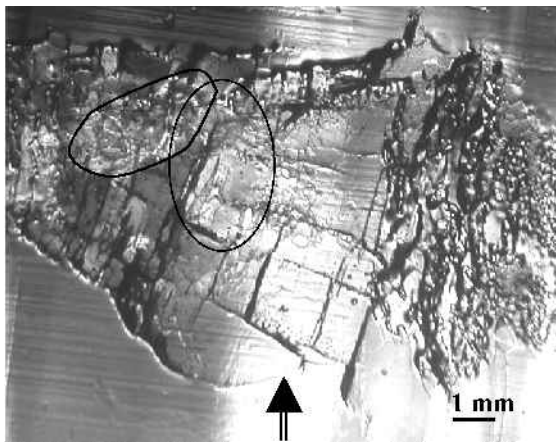


Fig. 5. Surface cracks observed through cross-polarized light on a moving slab (thick section) after a test at 10^{-4} m s^{-1} , with a normal force of 47 kg m s^{-2} . The grain-size is $< 4\text{ mm}$. Note the near-orthogonal extensions (arrow) to the main cracks.

deviation reported in Figure 4 is then related to the minimum and maximum over these F_t values.

3.1. Friction coefficient for fresh-water columnar ice

Figure 4 shows the results obtained for μ as a function of sliding velocity. Also shown are the results from Kennedy and others (2000) for fresh-water granular ice of 4 mm grain-size, for the same test temperature. If we assume uniform contact area, as did Kennedy and others (2000), a normal stress of 0.01 MPa was applied during our experiments, while a normal stress of 0.02 MPa was applied during the experiments of Kennedy and others (2000). Since normal stress, at least for our experimental conditions, does not appear to influence the results (Kennedy and others, 2000), the comparison is valid. Note that at the higher velocities where we performed at least four tests at each speed, the two sets of data overlap reasonably well. A significant difference is observed only at the two lowest velocities where we ran fewer tests. This difference may be the result of insufficient data.

Thus, under the conditions of the present study, it appears reasonable to conclude that the friction behavior of columnar S2 fresh-water ice is similar to that of fresh-water

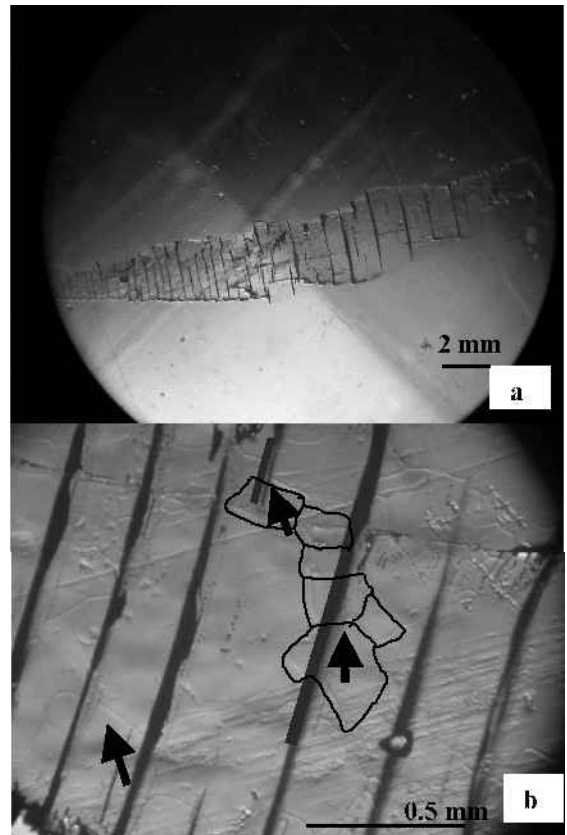


Fig. 6. Surface cracks observed in a moving slab after a test at 10^{-5} m s^{-1} , with a normal force of 25 kg m s^{-2} . The grain-size range is 6–8 mm. (a) Cracks observed through cross-polarized light; (b) higher magnification showing high-angle grain boundaries intersecting cracks (indicated by arrows).

granular ice and, by implication (Kennedy and others 2000), to that of columnar S2 saline ice.

3.2. Surface damage: preliminary observations

Frictional sliding is generally accompanied by the creation of damage. Figure 5 shows surface cracks in a sample of ice sliding at 10^{-4} m s^{-1} under a normal load of 47 kg m s^{-2} . In this particular case, the average column diameter was around 4 mm. Figure 6 shows damage created at 10^{-5} m s^{-1} under a normal load of 25 kg m s^{-2} . Both figures were taken from the surface of the mobile slab. Similar damage features were observed on the stationary slab.

The following observations are noteworthy:

- (i) The cracks were generally oriented perpendicular to the direction of sliding and were located in small regions ($< 5\text{ mm}$ wide). They appeared in several positions during the test. The crack zone corresponds to a stronger contact zone, and as a result we observed a rotation of the stationary blocks about the horizontal axis perpendicular to the ice blocks. The cracks formed at the center of rotation where the sliding velocity was the one imposed. The rotation reveals that the real area of contact was not homogeneous over the whole sample, but changed during sliding. This must account for some variation of the friction force, but is not taken into account as the area considered for the calculation is the surface of the moving slab. The cracks shown in Figure 6a, for instance, formed after the block had

rotated by $\sim 45^\circ$, judging from the orientation of the grain boundary that runs diagonally across the image.

- (ii) Cracks formed only below a given threshold in displacement rate, depending upon the normal force. For a normal force of 25 kg m s^{-2} , damage occurred at speeds lower than 10^{-4} m s^{-1} , while for a force of 47 kg m s^{-2} surface cracks developed at speeds as high as 10^{-3} m s^{-1} . Above this threshold velocity (for each normal force), the surface was rather opaque after sliding. The opacity was probably related to a more homogeneous repartition of microcracks, due to a more homogeneous contact area, creating a “crushed-ice” like surface.
- (iii) Cracking, at least at the higher speed and load (10^{-4} m s^{-1} , 47 kg m s^{-2} ; Fig. 5), appears to have been accompanied by other processes as well. This point was deduced from localized changes in crystal orientation within the damaged zone, evident from the presence of millimeter-sized regions of interference colors (blue, green, yellow; not shown in the black-and-white image) that we observed within the two encircled parts of Figure 5, and from what may be the result of partial melting (large, rough-looking zone in the righthand part of Figure 5).
- (iv) The crack depth was generally $< 600 \mu\text{m}$, at least for the case shown in Figure 6. We measured it by shaving the surface carefully with the microtome, until the elimination of the cracks. The average distance between the cracks (Fig. 6) was $0.5 \pm 0.2 \text{ mm}$.
- (v) Secondary cracks occurred on each side of the damage zone (e.g. arrow in Fig. 5) nearly perpendicular to many of the main cracks.
- (vi) High-angle grain boundaries, etched through preferential sublimation of the specimen when in the cold room and faintly visible in Figure 6b, formed within the damage zone. These boundaries were not observed outside this zone, implying that they are deformation features. They are indicative of sliding-induced recrystallization, and are reminiscent of similar features observed by Barnes and others (1971) when sliding a monocrystal of ice over granite. It is important to note that the grain boundaries were intersected by cracks (Fig. 6b), for this shows that the recrystallization occurred dynamically (i.e. during deformation) before crack formation.

None of the surface features (cracks, recrystallized grains) was seen on the as-microtomed surface before testing.

4. ANALYSIS AND DISCUSSION

To summarize, we found that the kinetic coefficient of friction of S2 fresh-water ice on itself is essentially the same as that found by Kennedy and others (2000) for granular fresh-water ice and for S2 saline ice sliding on themselves, all at relatively low sliding velocities. This means that the underlying physical processes are rather insensitive to the initial microstructure of the ice and that the friction coefficient is controlled largely by processes intrinsic to the surface regions. These processes are dominated by dislocation creep at the lowest speeds, by fracture at intermediate speeds and by surface melting at the highest speeds, and are discussed by Kennedy and others (2000).

The more novel aspect of our work is the evidence for surface cracking and for dynamic recrystallization followed by grain growth. We thus focus on this aspect in the following discussion.

4.1. Crack initiation

We assume that the sliding surface contained initial stress concentrators of size c_0 , and that, under frictional drag, cracks initiated from such concentrators when the mode-I stress intensity factor K_I reached a critical level, governed by fracture toughness K_{Ic} . The problem is essentially one of an edge crack in a stress gradient. In that case, $K_I \sim 1.12 \sigma_t \sqrt{\pi c_0}$ (Sih, 1973) where σ_t is the effective tensile stress. When c_0 is small compared with the contact radius, the tensile stress is nearly constant, and so we assume that σ_t is the tensile stress at the surface. Were the points of contact spherical in shape, then the cracks would have been curved, owing to the action of both Hertzian and sliding stresses. In that case, the model of Kong and Ashby (1992) for a spherical slider on a flat plate could have been applied. However, our cracks are relatively straight (Figs 5 and 6), and this implies line-like instead of spherical contact. We thus assume cylindrically shaped contact points. In this case, $\sigma_t = 2\mu p$ (Zambelli and Vincent 1998), where p is the normal pressure and is given as $p = 2P/(\pi a l)$ where P is the applied load, $2a$ is the contact width and l is the contact length. The criterion for initiating a crack from the tip of a stress concentrator during sliding may then be expressed as:

$$\mu P = \frac{al}{4.5} \sqrt{\frac{\pi}{c_0}} K_{Ic}. \quad (1)$$

This criterion is consistent with the observation in paragraph (ii) from section 3.2 in that the product of the friction coefficient and the normal load at the sliding speed required for cracking is about the same in the two cases cited. That is, at 10^{-5} m s^{-1} and $P = 25 \text{ kg m s}^{-2}$ where $\mu = 0.4$ (Fig. 4) the product $\mu P = 10 \text{ kg m s}^{-2}$, and at 10^{-4} m s^{-1} and $P = 47 \text{ kg m s}^{-2}$ where $\mu = 0.2$ (Fig. 4) $\mu P = 9.4 \text{ kg m s}^{-2}$. The criterion is more difficult to evaluate on other grounds. We do not know the contact area, so we are unable to calculate very well the crack-opening stress intensity factor. Thus, it is difficult to determine with much confidence the size of the stress concentrator from which the cracks initiated. Our best order-of-magnitude estimate is $c_0 \sim 0.1 \mu\text{m}$. This was obtained by (i) taking $l \sim 1 \text{ mm}$ and $a = 2\sqrt{LR/\pi E}$ (Zambelli and Vincent 1998), where L is the line load per unit length, given by $L = P/l$, R is the radius of the cylindrical contact and E is Young’s modulus of ice; (ii) assuming $R \sim 1 \text{ mm}$; and (iii) using $E = 10 \text{ GPa}$ (Gammon and others 1983), $K_{Ic} = 0.1 \text{ MPa m}^{1/2}$ (Dempsey 1996) and $\mu P = 10 \text{ kg m s}^{-2}$. Barring concern about the appropriate value of the contact radius, we are encouraged by the fact that, in estimating sub-micrometer-sized defects — produced either during the initial preparation of the surface or during the initial stages of sliding — the model gives a reasonable result.

On crack spacing, s , it appears that this factor is related to the crack depth, d (Fig. 7), judging from the similarity of their values ($s \sim 0.5 \text{ mm}$, $d < 600 \mu\text{m}$; paragraph (iv) in section 3.2). The spacing presumably reflects the distance ahead of a free surface (crack) at which the near-surface tensile stress, when concentrated, reaches a value sufficiently high to initiate a new crack. The crack depth itself is limited by strain energy.

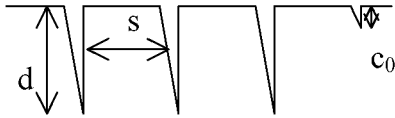


Fig. 7. Sketch of the crack feature. S is the distance between cracks, d is the crack depth and c_0 is the height of initial stress concentrators.

The other point to note is the similarity between the sliding-induced cracks we report here and the sets of secondary cracks that emanate from cracked grain boundaries which slide within bulk specimens loaded under far-field compression (see Schulson and others 1999, fig. 2c). This similarity, we believe, reflects the role of friction both in the creation of surface damage, as discussed above, and in brittle compressive failure, as mentioned in the Introduction.

4.2. Dynamic recrystallization on the surface

New nuclei form in localized regions of high dislocation density and hence of high strain energy, and then grow via grain boundary migration (Humphreys and Hatherly, 1996). If we assume a spherical nucleus of radius r , then a free energy ΔG_n per unit volume is needed to start the process of grain growth. This is given by (Duval and others, 1983):

$$\Delta G_n = \frac{2\gamma_{GB}}{r}, \quad (2)$$

where γ_{GB} is the grain boundary energy. Taking $\gamma_{GB} = 0.06 \text{ J m}^{-2}$ and $r = 0.1 \text{ mm}$ (upper bound for nucleus in ice; Duval and others, 1983), we find that $\Delta G_n \approx 10^3 \text{ J m}^{-3}$. This driving force is the minimum available to induce grain growth after nucleation. At the temperature of our experiments, such a driving force gives a grain growth rate of approximately $A_{gb}(-10^\circ\text{C}) \approx 7 \times 10^{-14} \text{ m}^2 \text{ s}^{-1}$ (Duval and others, 1983).

How does this rate compare with that derived from our experiment? We measured an average grain-size of 0.3 mm within the recrystallized zone (Fig. 6b). Assuming that the recrystallization occurred during sliding when the two samples were in contact, then for a sliding speed of 10^{-5} m s^{-1} and a maximum length of contact of 50 mm (size of the moving block), the upper bound for the duration of contact is $5 \times 10^3 \text{ s}$. A lower bound of the measured area growth rate is then $A_{gb,m} = \pi(0.15 \times 10^{-3}) / (5 \times 10^{-11}) \approx 10^{-11} \text{ m}^2 \text{ s}^{-1}$. This rate is about two orders of magnitude higher than that expected from Duval and others (1983). However, owing to frictional heating, the temperature of the contact area was probably higher than the room temperature (-10°C). We estimated the temperature increase by equating the work of friction to adiabatic heating, from the relationship:

$$\Delta T = \frac{F\Delta x}{C_p\rho V}, \quad (3)$$

where $F = \mu P$ is the frictional force on the surface, Δx is the sliding distance, C_p is the specific heat capacity ($1.962 \text{ kJ K}^{-1} \text{ kg}^{-1}$ at -10°C) and ρ the density of ice (917 kg m^{-3}); V is the volume of the contact zone and is given by $V = l\delta\Delta x$, where again l is the length of the contact ($l \sim 1 \text{ mm}$), and δ is the depth of deformation ($\delta \sim 1 \text{ mm}$). Thus, for $\mu P = 10 \text{ kg m s}^{-2}$, the temperature of the sliding surface was probably about -5°C . At this temperature, the grain growth rate is much higher than at -10°C , and from Duval and others (1983) is expected to be $A_{gb}(-5^\circ\text{C}) \approx 7 \times 10^{-11} \text{ m}^2 \text{ s}^{-1}$. The

growth rate we deduced from our experiment is thus in reasonably good agreement with expectation.

4.3. Surface melting?

We do not know whether melting played a role here. The appearance of the rubbed surface noticed in paragraph (iii) in section 3.2 suggests that it may have. If it did, then the contact pressure would have had to lower the surface temperature by $\sim 5 \text{ K}$ (over the frictional heating) and this would imply local pressures of $\sim 64 \text{ MPa}$ as well as true contact areas a factor of ~ 6400 lower than the apparent area. More work is needed to evaluate this possibility.

5. CONCLUSIONS

The present study on the friction of fresh-water S2 ice sliding slowly against itself at -10°C complements that of Kennedy and others (2000). Comparison shows no major difference in the kinetic friction coefficient between the columnar fresh-water S2 ice of this study and either the granular fresh-water ice or the columnar S2 saline ice studied by Kennedy and others (2000).

Friction-induced surface damage on the sliding samples includes localized cracking and recrystallization on a macroscopic scale. Cracking is consistent with a simple criterion based upon fracture mechanics, and recrystallization and grain growth are consistent with the model of Duval and others (1983).

ACKNOWLEDGEMENTS

We would like to acknowledge F. Kennedy for valuable discussions, and two anonymous reviewers for their thoughtful comments. We also acknowledge S. J. Jones, the Scientific Editor, for his help. This work was supported by U.S. National Oceanographic and Atmospheric Administration (NOAA) grant No. NA17RP1400.

REFERENCES

- Barnes, P., D. Tabor and J. C. F. Walker. 1971. The friction and creep of polycrystalline ice. *Proc. R. Soc. London, Ser. A*, **324**(1557), 127–155.
- Bowden, F. P. and T. P. Hughes. 1939. The mechanism of sliding on ice and snow. *Proc. R. Soc. London, Ser. A*, **172**(949), 280–298.
- Dempsey, J. P. 1996. Scale effects on the fracture of ice. In Arsenault, R. J. and 6 others, eds. *The Johannes Weertman Symposium, 5–9 February 1996, Anaheim, California*. Warrendale, PA, The Minerals, Metals and Materials Society, 351–362.
- Duval, P., M. F. Ashby and I. Anderman. 1983. Rate-controlling processes in the creep of polycrystalline ice. *J. Phys. Chem.*, **87**(21), 4066–4074.
- Evans, D. C. B., J. F. Nye and K. J. Cheeseman. 1976. The kinetic friction of ice. *Proc. R. Soc. London, Ser. A*, **347**(1651), 493–512.
- Gammon, P. H., H. Kieft and M. J. Clouter. 1983. Elastic constants of ice samples by Brillouin spectroscopy. *J. Phys. Chem.*, **87**(21), 4025–4029.
- Hopkins, M. A., W. D. Hibler, III and G. M. Flato. 1991. On the numerical simulation of the sea ice ridging process. *J. Geophys. Res.*, **96**(C3), 4809–4820.
- Hopkins, M. A., J. Tuhkuri and M. Lensu. 1999. Rafting and ridging of thin ice sheets. *J. Geophys. Res.*, **104**(C6), 13,605–13,613.
- Humphreys, F. J. and M. Hatherly. 1996. *Recrystallization and related annealing phenomena*. Oxford, etc., Pergamon Press.
- Kennedy, F. E., E. M. Schulson and D. E. Jones. 2000. The friction of ice on ice at low sliding velocities. *Philos. Mag. A*, **80**(5), 1093–1110.
- Kong, H. and M. F. Ashby. 1992. Wear mechanisms in brittle solids. *Acta Metall. Mater.*, **40**(11), 2907–2920.
- Michel, B. and R. O. Ramseier. 1971. Classification of river and lake ice. *Can. Geotech. J.*, **8**(1), 36–45.
- Schulson, E. M. 2001. Brittle failure of ice. *Eng. Frac. Mech.*, **68**(17–18), 1839–1887.
- Schulson, E. M., D. Iliescu and C. E. Renshaw. 1999. On the initiation of shear

- faults during brittle compressive failure: a new mechanism. *J. Geophys. Res.*, **104**(B1), 695–705
- Sih, G. C. 1973. *Handbook of stress intensity factors for researchers and engineers*. Bethlehem, PA, Lehigh University. Institute of Fracture and Solid Mechanics.
- Tusima, K. 1977. Friction of a steel ball on a single crystal of ice. *J. Glaciol.*, **19**(81), 225–235.
- Zambelli, G. and L. Vincent. 1998. *Matériaux et contacts*. Lausanne, Presses Polytechniques Universitaires Romandes.

MS received 3 September 2002 and accepted in revised form 29 April 2003